

## Evidence for the saturation of the Froissart bound

M. M. Block

*Department of Physics and Astronomy, Northwestern University, Evanston, Illinois 60208, USA*

F. Halzen

*Department of Physics, University of Wisconsin, Madison, Wisconsin 53706, USA*

(Received 18 May 2004; published 11 November 2004)

It is well known that fits to high energy data cannot sharply discriminate between asymptotic  $\ln s$  and  $\ln^2 s$  behavior of total cross section. We show that this is no longer the case when we impose the condition that the amplitudes also describe, on average, low energy data dominated by resonances. We demonstrate this by fitting real analytic amplitudes to high energy measurements of the  $\gamma p$  total cross section, for  $\sqrt{s} \geq 4$  GeV. We subsequently require that the asymptotic fit smoothly join the  $\sqrt{s} = 2.01$  GeV cross section described by Damashek and Gilman [M. Damashek and F. J. Gilman, Phys. Rev. D **1**, 1319 (1970).] as a sum of Breit-Wigner resonances. The results strongly favor the high energy  $\ln^2 s$  fit of the form  $\sigma_{\gamma p} = c_0 + c_1 \ln(\nu/m) + c_2 \ln^2(\nu/m) + \beta_{\mathcal{P}'} / \sqrt{\nu/m}$ , basically excluding a  $\ln s$  fit of the form  $\sigma_{\gamma p} = c_0 + c_1 \ln(\nu/m) + \beta_{\mathcal{P}'} / \sqrt{\nu/m}$ , where  $\nu$  is the laboratory photon energy. This evidence for saturation of the Froissart [M. Froissart, Phys. Rev. **123**, 1053 (1961).] bound for  $\gamma p$  interactions is confirmed by applying the same analysis to  $\pi p$  data using vector meson dominance.

DOI: 10.1103/PhysRevD.70.091901

PACS numbers: 11.80.-m

The Froissart bound [1] says that the high energy cross section for the scattering of hadrons is bounded by  $\sigma \sim \ln^2 s$ , where  $s$  is the square of the cms energy. This fundamental result is derived from unitarity and analyticity by Froissart [1], who states: “At forward or backward angles, the modulus of the amplitude behaves at most like  $s \ln^2 s$ , as  $s$  goes to infinity. We can use the optical theorem to derive that the total cross sections behave at most like  $\ln^2 s$ , as  $s$  goes to infinity.” In this context, saturating the Froissart bound refers to an energy dependence of the total cross section rising no more rapidly than  $\ln^2 s$ .

The question as to whether any of the present day high energy data for  $\bar{p}p$ ,  $pp$ ,  $\pi^+p$ ,  $\pi^-p$ ,  $\gamma p$ , and  $\gamma\gamma$  cross sections saturate the Froissart bound has not been settled; one can not discriminate between asymptotic fits of  $\ln s$  and  $\ln^2 s$  using high energy data only [2]. We here point out that this ambiguity is resolved by requiring that the fits to the high energy data smoothly join the cross section and energy dependence obtained by averaging the resonances at low energy. We show that only fits to the high energy data behaving as  $\ln^2 s$  that smoothly join to the low energy data on  $\gamma p$  total cross sections in the resonance region, can adequately describe the highest energy points (the smoothness constraint is analogous to the duality requirement imposed by Igi [3]). For the low energy cross sections we use a convenient parametrization by Damashek and Gilman [4] of the forward Compton scattering amplitudes, which yields a very accurate description of the low energy data. It provides us with a best fit in the energy region  $2m\nu_0 + m^2 \leq \sqrt{s} \leq 2.01$  GeV using five Breit-Wigner resonances and a 6th order polynomial in  $(\sqrt{s} - \sqrt{s_{\text{threshold}}})$ . Here  $\nu_0 = m_\pi + m_\pi^2/m$  is the threshold and  $m$  the proton mass. Their result is shown in Fig. 1.

Following Block and Cahn [5], we write the crossing-even real analytic amplitude for high energy  $\gamma p$  scattering as [6]

$$f_+ = i \frac{\nu}{4\pi} \left\{ A + \beta [\ln(s/s_0) - i\pi/2]^2 + c s^{\mu-1} e^{i\pi(1-\mu)/2} - i \frac{4\pi}{\nu} f_+(0) \right\}, \quad (1)$$

where  $A$ ,  $\beta$ ,  $c$ ,  $s_0$ , and  $\mu$  are real constants. The variable  $s$  is the square of the c.m. system energy and  $\nu$  the laboratory momentum. The additional real constant  $f_+(0)$  is the subtraction constant at  $\nu = 0$  introduced in the singly-

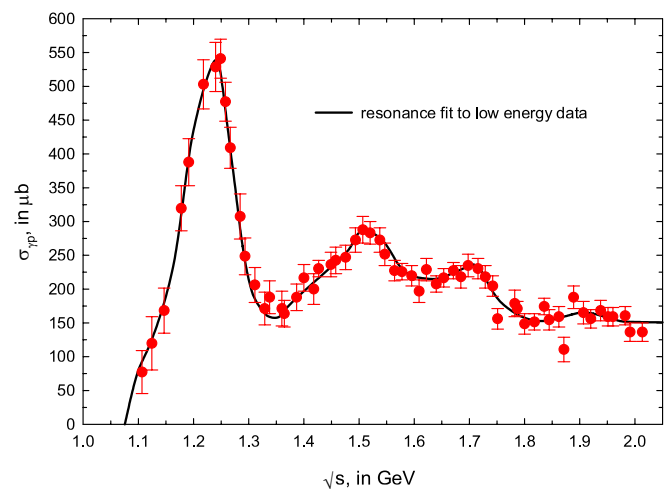


FIG. 1 (color online). The heavy line is a fit, by Damashek and Gilman [4], of the low energy  $\sigma_{\gamma p}$  data to a sum of five Breit-Wigner resonances plus a sixth-order polynomial background. The fitted value of  $\sigma_{\gamma p}$  at  $\sqrt{s} = 2.01$  GeV is  $151 \mu\text{b}$ .

subtracted dispersion relation [4] for the reaction  $\gamma + p \rightarrow \gamma + p$ . It is fixed in the Thompson scattering limit  $f_+(0) = -\alpha/m = -3.03\mu\text{b GeV}$ . Using the optical theorem, we obtain the total cross section

$$\sigma_{\gamma p} = A + \beta \left[ \ln^2 s/s_0 - \frac{\pi^2}{4} \right] + c \sin(\pi\mu/2) s^{\mu-1} \quad (2)$$

and  $\rho$ , the ratio of the real to the imaginary part of the forward scattering amplitude, given by

$$\rho = \frac{1}{\sigma_{\text{tot}}} \left\{ \beta \pi \ln s/s_0 - c \cos(\pi\mu/2) s^{\mu-1} + \frac{4\pi}{\nu} f_+(0) \right\}. \quad (3)$$

Introducing the definitions  $A = c_0 + \frac{\pi^2}{4} c_2 - \frac{c_1^2}{4c_2}$ ,  $s_0 = 2m^2 e^{-c_1/(2c_2)}$ ,  $\beta = c_2$  and  $c = \frac{(2m^2)^{1-\mu}}{\sin(\pi\mu/2)} \beta_{\mathcal{P}'}$ , Eq. (2) and Eq. (3) can, in the high energy limit  $s \rightarrow 2m\nu$ , be written as

$$\sigma_{\gamma p} = c_0 + c_1 \ln\left(\frac{\nu}{m}\right) + c_2 \ln^2\left(\frac{\nu}{m}\right) + \beta_{\mathcal{P}'} \left(\frac{\nu}{m}\right)^{\mu-1}, \quad (4)$$

$$\rho_{\gamma p} = \frac{1}{\sigma} \left\{ \pi 2c_1 + \pi c_2 \ln\left(\frac{\nu}{m}\right) - \cot(\pi\mu/2) \beta_{\mathcal{P}'} \left(\frac{\nu}{m}\right)^{\mu-1} + \frac{4\pi}{\nu} f_+(0) \right\}. \quad (5)$$

This transformation linearizes Eq. (4) in the real coefficients  $c_0$ ,  $c_1$ ,  $c_2$ , and  $\beta_{\mathcal{P}'}$ , convenient for a straightforward  $\chi^2$  fit to the experimental  $\gamma p$  total cross sections. Throughout we will use units of  $\nu$  in GeV and cross section in  $\mu\text{b}$ .

Our strategy is to constrain the high energy fit with the precise low energy fit at  $\sqrt{s} \leq 2.01$  GeV, which is the energy where Damashek and Gilman [4] join the energy region dominated by resonances to a Regge fit,  $a + b/\sqrt{\nu/m}$ . They find that the cross section at  $\sqrt{s} = 2.01$  is  $151 \mu\text{b}$  and the slope  $d\sigma_{\gamma p}/d(\nu/m)$  is  $-b/(\nu/m)^{1.5}$ , or  $-15.66$  in  $\mu\text{b}$  units. Using the asymptotic expression of

Eq. (4), we obtain two constraints

$$\beta_{\mathcal{P}'} = 73.0 + 2.68c_1 + 3.14c_2, \quad (6)$$

$$c_0 = 151 - 0.586c_1 - 0.343c_2 - 0.746\beta_{\mathcal{P}'}, \quad (7)$$

by matching the values of the slope and the cross section, respectively. Unless stated otherwise, both constraints are used in our  $\chi^2$  fitting procedure.

We next fit the asymptotic form of Eq. (4) to the high energy data in the energy range  $4 \leq \sqrt{s} \leq 210$  GeV. The lower energy data are from the Particle Data Group[7]; the high energy points at  $\sqrt{s} = 200$  and  $\sqrt{s} = 209$  GeV are from the H1 Collaboration [8] and Zeus [9] Collaboration, respectively. The results are summarized in Table I. For Fit 1, the data are fitted with a  $\ln^2(\nu/m)$  energy dependence imposing constraints Eq. (6) and Eq. (7). We thus obtain fitted values for  $c_1$  and  $c_2$ , which then determine  $c_0$  and  $\beta_{\mathcal{P}'}$ . The fit is excellent, yielding a total  $\chi^2$  of 50.34 for 61 degrees of freedom, with a fit probability of 0.83. The fit is shown as the solid line in Fig. 2. In order to verify that the data discriminates between a  $\ln^2(\nu/m)$  fit and a  $\ln(\nu/m)$  fit, we made Fit 3 assuming a  $\ln(\nu/m)$  energy dependence, i.e.,  $c_2 = 0$ . After fitting  $c_1$ , we determine  $c_0$  and  $\beta_{\mathcal{P}'}$  from the constraint equations. The fit is poor with a total  $\chi^2$  of 102.8 for 62 degrees of freedom. This corresponds to a chance probability of  $8.76 \times 10^{-4}$ . It is plotted as the dotted line in Fig. 2 and clearly underestimates the high energy cross section measurements. Finally, to test the stability of the  $\ln^2(\nu/m)$  fit, we relax the condition that the slopes of the low energy fit and the asymptotic fit are the same at  $\sqrt{s} = 2.01$  GeV, only imposing the cross section constraint of Eq. (7). Thus, in Fit 2, we fit  $c_1$ ,  $c_2$ , and  $\beta_{\mathcal{P}'}$ , which then determines  $c_0$ . This also yields a good fit, with a total  $\chi^2$  of 47.48, for 60 degrees of freedom, corresponding to a chance probability of 0.88. Fit 2 is shown as the dashed-dotted line in Fig. 2. It fits the data well, indicating stability of the procedure. Clearly, the constraints im-

TABLE I. The fitted results, where  $m$  is the proton mass and  $\nu$  is the laboratory photon energy.

Parameters	$\sigma \sim \log^2(\nu/m)$		$\sigma \sim \log(\nu/m)$
	Fit 1	Fit 2	Fit 3
	$c_0$ and $\beta_{\mathcal{P}'}$ constrained	$c_0$ constrained	$c_0$ and $\beta_{\mathcal{P}'}$ constrained
$c_0$ ( $\mu\text{b}$ )	105.64	92.5	84.22
$c_1$ ( $\mu\text{b}$ )	$-4.74 \pm 1.17$	$-0.46 \pm 2.88$	$4.76 \pm 0.11$
$c_2$ ( $\mu\text{b}$ )	$1.17 \pm 0.16$	$0.803 \pm 0.273$	—
$\beta_{\mathcal{P}'}$ ( $\mu\text{b}$ )	64.0	$78.4 \pm 9.1$	85.8
$\mu$	0.5	0.5	0.5
$\chi^2$	50.34	47.48	102.8
d.f.	61	60	62
$\chi^2/\text{d.f.}$	0.825	0.791	1.657
Probability	0.83	0.88	$8.76 \times 10^{-4}$

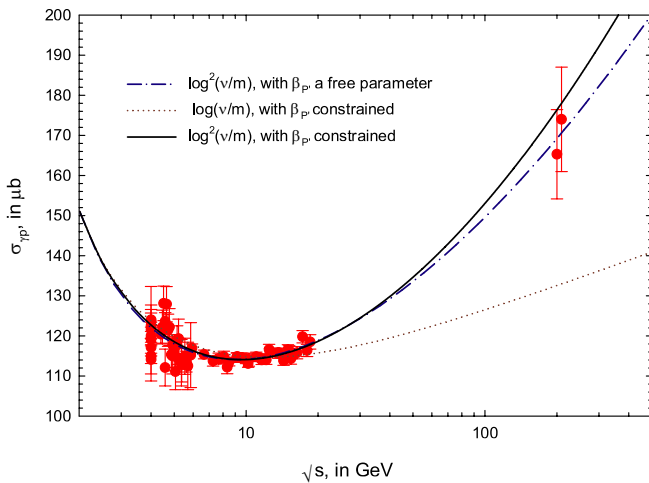


FIG. 2 (color online). The fitted  $\sigma_{\gamma p}$ , in  $\mu\text{b}$ , vs.  $\sqrt{s}$ , in GeV. The solid curve (Fit 1) is a  $\chi^2$  fit (Fit 1) of the high energy data of the form:  $\sigma_{\gamma p} = c_0 + c_1 \ln(\nu/m) + c_2 \ln^2(\nu/m) + \beta_{\mathcal{P}'} / \sqrt{\nu/m}$ , with both  $c_0$  and  $\beta_{\mathcal{P}'}$  constrained by Eq. (6) and Eq. (7). The constraints were found from a low energy fit to the resonance region and a Regge  $\mathcal{P}'$  trajectory [4]. The dot-dashed line is a  $\log^2(\nu/m)$  fit (Fit 2) that constrains  $c_0$  only, allowing  $\beta_{\mathcal{P}'}$  to be a free parameter in the fit. The dotted line (Fit 3), uses:  $\sigma_{\gamma p} = c_0 + c_1 \ln(\nu/m) + \beta_{\mathcal{P}'}/\sqrt{\nu/m}$ , with both  $c_0$  and  $\beta_{\mathcal{P}'}$  constrained by Eq. (6) and Eq. (7). The laboratory energy of the photon is  $\nu$  and  $m$  is the proton mass. The data used in all fits are the cross sections with  $\sqrt{s} \geq 4$  GeV. All fits pass through the low energy anchor point at  $\sqrt{s} = 2.01$  GeV, where  $\sigma_{\gamma p} = 151 \mu\text{b}$ . Fits one and three are further constrained to have the same slope as the low energy fit, at  $\sqrt{s} = 2.01$  GeV. Details of the three fits are given in Table I.

posed by the low energy data strongly restricts the asymptotic behavior [10].

In a recent paper, Igi and Ishida [3] have analyzed  $\pi^+ p$  and  $\pi^- p$  total cross sections using parametrizations of the form of Eq. (4), with both  $\ln(\nu/m)$  and  $\ln^2(\nu/m)$ . They derive two finite energy sum rules, which, when applied to the low energy data give two constraint equations. Subject to these constraints, they make asymptotic fits to the available high energy  $\pi^+ p$  and  $\pi^- p$  data. Their analysis also favors a  $\ln^2(\nu/m)$  behavior of the cross sections. In a vector meson dominance model (in the spirit of the quark model), the cross section  $\sigma_{\gamma p}$  is proportional to the crossing-even  $\pi p$  cross section,  $\sigma_{\pi p} = (\sigma_{\pi^+ p} + \sigma_{\pi^- p})/2$ . We can thus confront our results above with  $\sigma_{\pi p}$  data, renormalized by a factor 208 familiar from vector meson dominance phenomenology. The result is shown as the dashed line in Fig. 3. The agreement is excellent over a large energy interval—particularly, since the pion fit was derived using data only up to  $\sqrt{s} \approx 30$  GeV, whereas the plot in Fig. 3 extends to 300 GeV.

Finally, Block and Kaidalov [11] have suggested that factorization requires  $\rho_{nn} = \rho_{\gamma p}$ , and by extension,  $\rho_{\gamma p}$

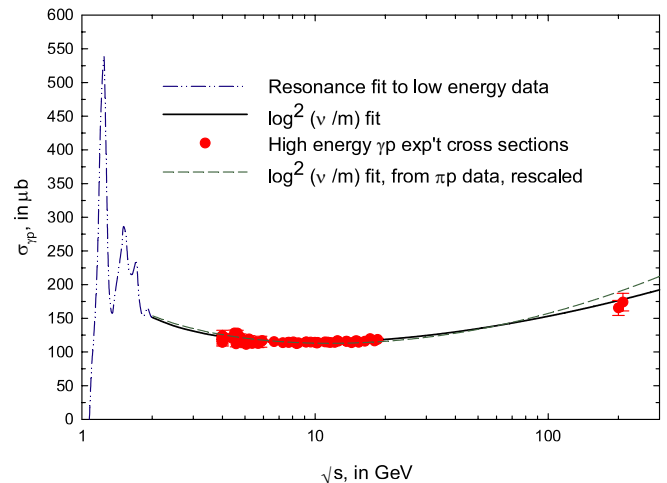


FIG. 3 (color online). The dashed-dot-dot line is a fit, by Damashek and Gilman [4], of the low energy  $\sigma_{\gamma p}$  data to a sum of five Breit-Wigner resonances plus a sixth-order polynomial background. The fit labeled  $\log^2(\nu/m)$ , the solid line, is a  $\chi^2$  fit (Fit 1) of the high energy data of the form:  $\sigma_{\gamma p} = c_0 + c_1 \ln(\nu/m) + c_2 \ln^2(\nu/m) + \beta_{\mathcal{P}'}/\sqrt{\nu/m}$ , with  $\beta_{\mathcal{P}'} = 64 \mu\text{b}$ . The laboratory energy of the photon is  $\nu$  and  $m$  is the proton mass. The dashed curve is from a  $\sigma_{\pi p} = c_0 + c_1 \ln(\nu/m) + c_2 \ln^2(\nu/m) + \beta_{\mathcal{P}'}/\sqrt{\nu/m}$  fit from Igi and Ishida [3], using their  $\pi p$  cross sections rescaled by a factor of  $1/208$ . The cross section curves join at  $\sqrt{s} = 2.01$  GeV, where the cross section is  $151 \mu\text{b}$ .

should be equal to  $\rho_{\pi p}$ , where  $\rho_{\pi p}$  is the even amplitude for  $\pi^+ p$  and  $\pi^- p$  scattering. To test this, we plot  $\rho_{\gamma p}$  as the solid curve in Fig. 4, using the parameters of Fit 1 in Eq. (5). To calculate  $\rho_{\pi p}$ , we have taken the  $\pi p$  fit parameters from Igi and Ishida[3] and have substituted

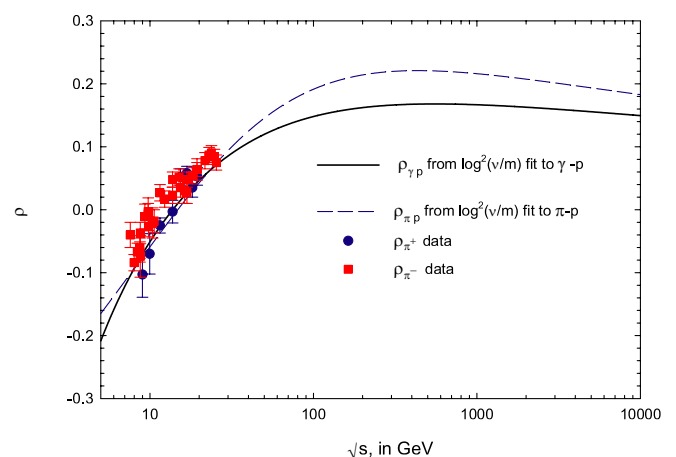


FIG. 4 (color online). A plot of  $\rho$  vs.  $\sqrt{s}$ , in GeV. The solid curve is  $\rho_{\gamma p}$ , calculated from the parameters of Fit 1. The dashed curve is  $\rho_{\pi p}$ , calculated from a  $\log^2 \nu$  fit to  $\pi^+ p$  and  $\pi^- p$  data [3]. The data shown are the experimental  $\rho$  values [7] for  $\pi^+ p$  and  $\pi^- p$ .

them in Eq. (5), where we have also set  $f_+(0) = 0$ . The dashed curve in Fig. 4 is  $\rho_{\pi p}$ . Also shown in Fig. 4 are the high energy experimental  $\rho$  data for  $\pi^+ p$  (the circles) and  $\pi^- p$  (the squares). We note that  $\rho_{\pi p} = (\rho_{\pi^+ p} + \rho_{\pi^- p})/2$ . The curves for  $\pi p$  and for  $\gamma p$  both reasonably describe the data, and essentially agree in the energy region below 30 GeV—again, we emphasize that the  $\pi p$  fit was only made for energies below 30 GeV.

In conclusion, we have demonstrated that the requirement that high energy cross sections smoothly interpolate into the resonance region strongly favors a  $\ln^2 s$  behavior of the asymptotic cross section—a behavior that saturates the Froissart bound. Using vector meson dominance (in

the spirit of the quark model), we demonstrate that our conclusions are also supported by  $\pi^+ p$  and  $\pi^- p$  data. Our analysis supports predictions of Large Hadron Collider cross sections that rely on the saturation of the Froissart bound.

We thank Martin Olsson for suggesting the advantage of doing the analysis with photoproduction data. The work of F.H. is supported in part by the U.S. Department of Energy under Grant No. DE-FG02-95ER40896 and in part by the University of Wisconsin Research Committee with funds granted by the Wisconsin Alumni Research Foundation.

- 
- [1] M. Froissart, Phys. Rev. **123**, 1053 (1961).
  - [2] M.M. Block, K. Kang, and A.R. White, Int. J. Mod. Phys. A **7**, 4449 (1992); The COMPETE Collaboration, J.R. Cudell *et al.*, Phys. Rev. D **65**, 074024 (2002). Some preference for  $\ln^2 s$  is found, but a  $\ln s$  energy dependence can not be statistically ruled out.
  - [3] Keiji Igi and Muneyuki Ishida, Phys. Rev. D **66**, 034023 (2002), and references therein.
  - [4] M. Damashek and F.J. Gilman, Phys. Rev. D **1**, 1319 (1970).
  - [5] M.M. Block and R.N. Cahn, Rev. Mod. Phys. **57**, 563 (1985).
  - [6] M.M. Block, Phys. Rev. D **65**, 116005 (2002).
  - [7] Particle Data Group, H. Hagiwara *et al.*, Phys. Rev. D **66**, 010001 (2002).
  - [8] H1 Collaboration, S. Aid *et al.*, Z. Phys. C **75**, 421 (1997).
  - [9] Zeus Collaboration, S. Chekanov *et al.*, Nucl. Phys. B **627**, 3 (2002). We use the error quoted by the authors, a combination of statistical and systematic errors. This is in the spirit of all of the other data quoted by the PDG [7] that we use.
  - [10] Numerical calculations have shown that our results are insensitive to the choice of  $\mu$  in Eq. (4) and Eq. (5), as well as the magnitude and slope of the cross section at the joining point,  $\sqrt{s} = 2.01$  GeV.
  - [11] M.M. Block and A. B. Kaidalov, Phys. Rev. D **64**, 076002 (2001).